Preliminary beam test results of an LGAD-based 5D sensor array for the next generation of space-borne experiments

Published by IOP Publishing for Sissa Medialab

Received: *February 17, 2026*
Accepted: *March 10, 2026*
Published: *April 22, 2026*

17th Topical Seminar on Innovative Particle and Radiation Detectors
Siena, Italy
15–19 September 2025

Preliminary beam test results of an LGAD-based 5D sensor array for the next generation of space-borne experiments

M. Mattiazzi[e,f,*] **G. Bigongiari**[a,b] **A. Bisht**[c] **M. Boscardin**[c,d] **E. Bossini**[b] **P. Brogi**[a,b] **M. Centis Vignali**[c,d] **G. Collazuol**[e,f] **G.-F. Dalla Betta**[d,g] **S. Giroletti**[h,i] **P. Maestro**[a,b] **P.S. Marrocchesi**[a,b] **N. Minafra**[l] **F. Morsani**[b] **L. Pancheri**[d,g] **L. Ratti**[h,i] **L. Stiaccini**[a] **and C. Vacchi**[h,i]

[a] *Dipartimento di Scienze Fisiche della Terra e dell'Ambiente, Universitá di Siena, Via Roma 56, I-53100 Siena, Italy*
[b] *INFN, Sezione di Pisa, Via Filippo Buonarroti 3, I-56127 Pisa, Italy*
[c] *Fondazione Bruno Kessler (FBK), Via Sommarive 18, I-38123 Trento, Italy*
[d] *INFN-TIFPA, Via Sommarive, 14, I-38123 Trento, Italy*
[e] *INFN, Sezione di Padova, Via Francesco Marzolo 8, I-35131 Padova, Italy*
[f] *Dipartimento di Fisica e Astronomia, Università di Padova, Via Francesco Marzolo 8, I-35131 Padova, Italy*
[g] *Dipartimento di Ingegneria Industriale, Università di Trento, Via Sommarive 9, I-38123 Trento, Italy*
[h] *Dipartimento di Ingegneria Industriale e dell'Informazione, Università di Pavia, Via Adolfo Ferrata 5, I-27100 Pavia, Italy*
[i] *INFN, Sezione di Pavia, Via Agostino Bassi 6, I-27100 Pavia, Italy*
[l] *Department of Physics and Astronomy, University of Kansas, Malott Hall, 1251 Wescoe Dr, Lawrence, KS 66045-7582, U.S.A.*

E-mail: marco.mattiazzi@pd.infn.it

[*] Corresponding author.

https://doi.org/10.1088/1748-0221/21/04/C04055

2026 JINST 21 C04055

Abstract: Direct measurements of the fluxes and relative abundances of charged cosmic rays carried out in space and on balloons, require the identification of the incoming particle and the measurement of its energy. Detectors in which tracking and particle-identification devices are operated in conjunction with calorimeters are affected by back-scattered radiation from the calorimeter, leading to a degradation of the charge resolution when the same charge-detector element is simultaneously hit by the incident cosmic ray and by the back-scattered component. To address these challenges, the ADA_5D project, funded by the Italian National Institute for Nuclear Physics (INFN), is developing an innovative detector, based on arrays of Low Gain Avalanche Diode (LGAD) pixels, for the simultaneous measurement of the incident particle position, charge, and timing (5D sensor) over a large dynamic range ($\sim$ 1000 MIP) and with sub-nanosecond time-of-flight (ToF) resolution. A large rejection power of the back-scattered background is expected, by leveraging ToF cuts on the late arrival of back-scattered signals on the charge detector with respect to the incident cosmic rays, and on the high granularity of the array. This paper reports the preliminary results of the first beam test of prototypal arrays of LGADs, developed for the ADA_5D project by FBK in Italy, and the performance of a first version of a low-power custom chip for timing and charge front-end processing. A preliminary analysis shows a timing resolution close to 100 ps and a charge resolution of the order of 0.1 charge units for light nuclei.

Keywords: Ion identification systems; Timing detectors; Particle tracking detectors (Solid-state detectors)

2026 JINST 21 C04055

Contents

1 Introduction

Direct measurements of the fluxes and relative abundances of charged cosmic rays in space require reliable identification of the incoming particle and an accurate determination of its energy. In current-generation balloon and space-borne instruments, charge identification is commonly achieved via dE/dx measurements in silicon detectors, which provide sufficient resolution and dynamic range to identify fully stripped nuclei from protons up to the iron group and beyond. This capability is a key feature for composition studies and for precision measurements of spectral features and elemental ratios over wide energy intervals.

Precision measurements of the lightest and most abundant species (protons and helium) set stringent requirements on both charge identification and control of systematics. In particular, AMS-02 measured the proton and helium fluxes [1] with high precision in rigidity up to the TV region, revealing a progressive hardening of the spectral indices at a few GV/nucleon and a non-trivial evolution of the p/He ratio. Calorimetric instruments have extended direct observations to higher energy: CALET [2, 3] and DAMPE [4] have reported proton measurements up to ~ 60 TeV and helium measurements up to ~ 250 TeV, highlighting additional spectral structures in the multi-TeV region. Looking further ahead, the MoonRay concept proposes long-term, large-acceptance measurements of cosmic-ray nuclei from the lunar surface to explore spectral features toward the knee region [5, 6].

However, a major limitation of state-of-the-art space-based detectors arises when silicon charge and tracking detectors are operated in conjunction with deep calorimeters. As the primary particle energy increases, secondary particles produced in the downstream calorimeter propagate upstream and generate additional ionization in the charge-sensitive planes. This back-scattered (backsplash) radiation can overlap in space and time with the signal from the primary particle, effectively contaminating the dE/dx measurement, broadening charge distributions, and increasing the probability of misidentification. Because the backsplash contribution typically grows with energy, the degradation becomes particularly relevant for the next generation of space experiments designed to extend composition measurements into the multi-TeV region and beyond.

A promising strategy to mitigate these effects and to enable new measurement capabilities is the development of *5D* detector layers, providing simultaneous measurements of position, charge, and time. Adding precise, layer-resolved timing to a granular charge detector allows one to exploit time-of-flight information to suppress late backsplash signals with respect to the prompt signal of the incident cosmic ray. In addition, timing information can improve track association in high-occupancy

2026 JINST 21 C04055

conditions and provide redundant particle-identification information to the instrument. For space applications, a per-layer timing resolution below ~ 200 ps is a key benchmark for efficient background rejection. In typical instrument geometries, backsplash secondaries traverse an additional path of order several tens of centimeters up to $\mathcal{O}(1\,\mathrm{m})$ with respect to the prompt particle, corresponding to delays of order $\mathcal{O}(1\text{–}3)$ ns. Hence, sub-nanosecond per-layer timing enables effective suppression of late components while preserving high charge-tagging efficiency.

Pixelated Low Gain Avalanche Diodes (LGADs) are an enabling technology for such 5D sensors, combining intrinsic gain with fast signal formation and excellent timing performance [7]. While LGAD development has been driven primarily by high-luminosity collider requirements, the comparatively milder radiation environment in space makes LGADs particularly attractive for large-area systems, provided that stringent constraints on power consumption, readout noise, and scalable front-end integration are met.

To address these challenges, the ADA_5D project, funded by the Italian National Institute for Nuclear Physics (INFN), is developing an innovative detector concept based on arrays of pixelated LGADs for the simultaneous measurement of position, charge over a wide dynamic range (~ 1000 MIP), and precise timing with sub-nanosecond time-of-flight resolution, in a scalable architecture suitable for $\mathcal{O}(1\ \mathrm{m}^2)$ coverage and low-power operation.

This paper reports the first beam test results of prototypal LGAD arrays (with 275 µm thickness) developed for ADA_5D and the performance of a first version of a low-power custom front-end chip for timing and charge processing. In detail, this work is focused primarily on charge performance, including new results for thick sensors (275 µm) such as element-separated spectra with Landau peak fits, correlations between LGAD charge and an external strip-tracker charge estimator, and an empirical characterization of response saturation versus Z^2. A concise section summarizes the timing performance of the sensors and of the front-end prototype, and the conclusions outline the next steps toward optimizing the detector and readout for future space-borne applications.

2 ADA_5D detector first prototype at Beam Test 2024

The ADA_5D detector concept is based on 3×3 mm^2 pixelated LGAD sensors, chosen as a compromise between granularity and input capacitance. In detail, the former improve the mitigation of back-scattering pile-up on a single channel, while the latter is essential to limit noise and therefore to preserve timing capabilities.

The LGAD devices under test have been produced by FBK (Fondazione Bruno Kessler, Trento) and they can be divided into two main categories: thin sensors (150 µm) and thick sensors (275 µm). The devices in each category span multiple layout variants based on guard-ring configurations and inter-pixel distances, as detailed in ref. [8]. The first ADA_5D beam test was carried out at the CERN SPS North Area (H4 beam line) during the 2024 winter campaign, using secondary ions produced by fragmentation of a primary Pb beam at 330 GeV/c per unit charge. The experimental apparatus combined:

- multiple layers of LGAD pixel devices under test (DUTs) instrumented for charge measurements and embedded in a silicon tracking system;
- a silicon strip tracker and silicon pixelated planes providing track reconstruction and an external charge reference;
- external scintillator triggers upstream and downstream of the setup.

2026 JINST 21 C04055

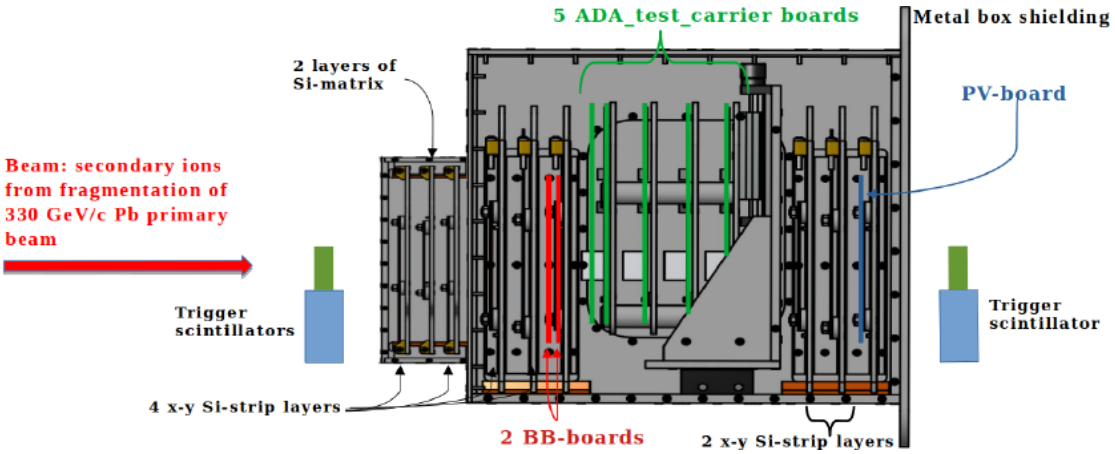

Figure 1. Beam-test apparatus at the CERN SPS North Area (H4) during the 2024 winter campaign. The setup combines the silicon tracking and external charge-tagging planes with multiple LGAD DUT layers and the dedicated readout systems used for charge, fast timing, and front-end characterization. Reproduced from [8].

A schematic of the beam-test apparatus is shown in figure 1.

A shielding enclosure hosted the DUTs and the tracking system, while waveform digitizers (high-bandwidth oscilloscopes) were used for the analog timing channels of the BB and PV boards.

Three complementary readout systems were used during the beam test: (i) a high-dynamic-range readout (based on the VA14-HDR ASIC [9]) integrated with the tracker DAQ for charge studies; (ii) dedicated fast timing boards (BB boards) instrumented for high-bandwidth waveform acquisition for sensor timing studies; (iii) a prototype ADA_5D front-end ASIC (version 0) mounted on a dedicated board (PV board) enabling access to multiple analog stages of one readout channel.

The ADA_5D v0 channel implements a trilinear charge sensitive amplifier with dynamic signal compression, followed by an RC-CR shaper with selectable shaping time, a fast discriminator, and a Time-to-Amplitude Converter (TAC) with selectable full-scale range. The TAC architecture and low-power design approach are discussed in dedicated electronics publications [10, 11].

3 Charge analysis

As a first step, tracks are reconstructed using the silicon strip planes after an off-line alignment procedure. Quality cuts select through-going, single-track events and suppress interactions inside the setup. The reconstructed impact point is used to associate the track to the corresponding LGAD pixel channel, enabling pixel type response studies and reducing the systematics due to pile-up events.

For charge studies, we use the VA-HDR readout amplitude after pedestal subtraction and channel equalization as a raw charge, denoted as Q_{LGAD} (in ADC units). In the following, the notation Z_{LGAD} is reserved to a reconstructed charge estimator expressed in *charge units*, obtained by calibrating Q_{LGAD} against an external charge tag and by accounting for the approximately quadratic scaling of the average ionization energy loss with the nuclear charge ($Q \propto Z^2$) and taking into account the relativistic rise.

The elemental-peak widths reported in this paper are extracted from fits to the Q_{LGAD} spectra. The ratio

$$R = \frac{\sigma_Q}{\mathrm{MPV}_Q} \tag{3.1}$$

2026 JINST 21 C04055

Table 1. Landau-component fit parameters for thick (275 µm) sensors in the light-ion region. MPV and σ_Q refer to the raw observable Q_{LGAD} (ADC units). The relative width $R = \sigma_Q/\mathrm{MPV}_Q$ characterizes the fractional spread of Q_{LGAD}. An approximate charge resolution in charge units, σ_Z, is obtained from eq. (3.2) under the first-order approximation $Q \propto Z^2$.

Element	Z	MPV (adu)	σ_Q (adu)	$R = \sigma_Q/\mathrm{MPV}_Q$	σ_Z (c.u.)
He	2	265.3 ± 0.7	39.0 ± 0.8	0.15	0.15
Li	3	566 ± 3	68 ± 5	0.12	0.18
Be	4	950 ± 9	120 ± 9	0.13	0.25
B	5	1390 ± 12	185 ± 15	0.13	0.33
C	6	1933 ± 17	239 ± 14	0.12	0.37

quantifies the relative width of the raw observable Q_{LGAD} and provides a detector-level figure of merit that is weakly dependent on the absolute calibration scale. In detail, each elemental peak is described with an independent Landau component within a multi-peak fit, allowing the extraction of the most probable value (MPV) and an effective width σ_Q in Q_{LGAD} units. The fit parameters extracted from the thick-sensor dataset in the light-ion region are summarized in table 1. A conversion to a resolution in charge units, σ_Z, can be obtained by standard error propagation once a calibration curve $Q(Z)$ is specified. For light ions and as a first-order approximation in the region where $Q \propto Z^2$, one obtains

$$\frac{\sigma_Z}{Z} \simeq \frac{1}{2}\frac{\sigma_Q}{Q} \quad \Rightarrow \quad \sigma_Z \simeq \frac{Z}{2} R. \tag{3.2}$$

This approximation is used below to provide an order-of-magnitude estimate of the charge resolution in charge units for light nuclei.

3.1 Thick sensors (275 µm): charge spectra and peak separation

Figure 2 shows the reconstructed LGAD charge spectrum for thick (275 µm) sensors after track-based selection of through-going events and pixel association. In the light-ion region, distinct peaks corresponding to He, Li, Be, B and C are clearly resolved.

From these fits, the relative width of the raw charge is $R \simeq 0.12$–0.15 for He-C. Using eq. (3.2), this corresponds to an approximate charge resolution in charge units of $\sigma_Z \simeq 0.15$ (He), ~ 0.18 (Li), increasing up to ~ 0.37 (C). The separation power between adjacent peaks, estimated as $S_{i,i+1} = |\mathrm{MPV}_{i+1} - \mathrm{MPV}_i|/\sqrt{\sigma^2_{Q,i} + \sigma^2_{Q,i+1}}$, ranges from ~ 3.8 (He-Li) down to ~ 1.8 (B-C), demonstrating the capabilities of charge identification for light nuclei and validating the use of pixelated LGADs for backsplash-mitigation studies. While the results above refer to a single instrumented LGAD layer, the ADA_5D concept foresees multiple layers in a stack. After channel equalization and track-based path-length corrections, a combined charge estimator built from N independent layer measurements can reduce the statistical component of the charge uncertainty approximately as $\sigma_Z^{(\mathrm{comb})} \simeq \sigma_Z/\sqrt{N}$. In addition to this variance reduction, the redundancy across layers enables consistency checks and outlier rejection, which is expected to further mitigate the impact of localized back-scatter hits on charge identification.

To validate the LGAD-based charge estimator and quantify linearity and saturation effects, figure 3 shows the event-by-event correlation between the LGAD observable and the external strip-tracker

2026 JINST 21 C04055

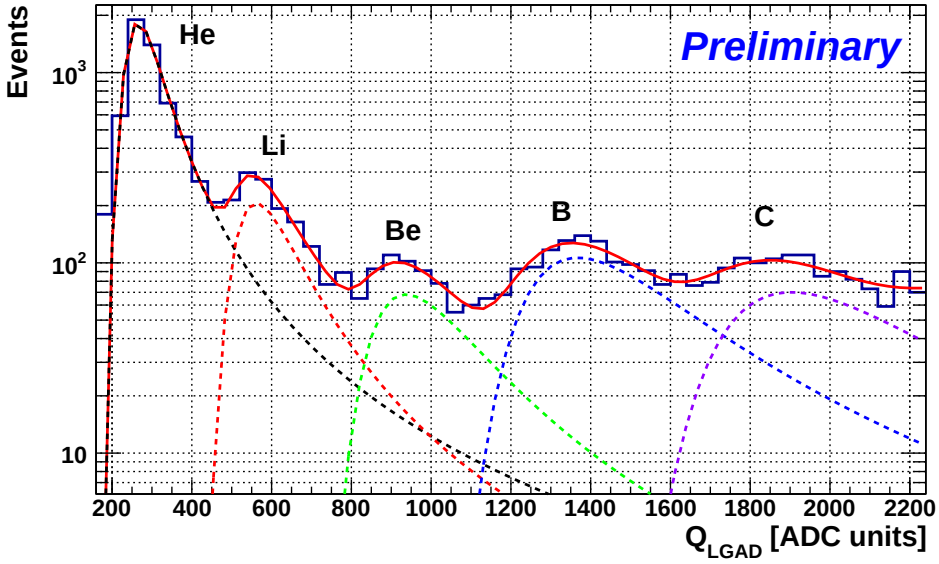

Figure 2. Reconstructed LGAD charge spectrum for thick (275 µm) sensors in the light-ion region, showing separated peaks for He, Li, Be, B and C. The red curves indicate the multi-Landau peak fit, while the dotted lines represent the individual fit component for each element.

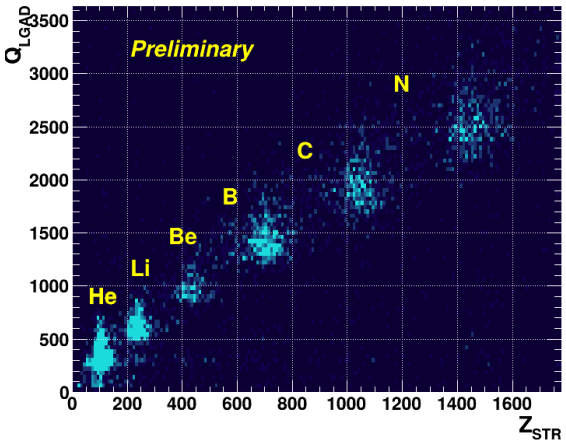

Figure 3. Correlation between LGAD-based reconstructed charge and external charge estimator from the silicon strip tracker (STR) for thick 275 µm sensors.

estimator Z_{STR}. The correlation exhibits distinct bands as a function of the external STR charge estimator and demonstrates that light ions can be distinguished using the LGAD pixels with non-negligible discrimination power. In addition, the correlation provides a cross-check of the LGAD observable against the independent STR charge tag, enabling data-driven studies of systematic effects such as track path-length corrections, hit multiplicity, and cross-talk.

3.2 Charge linearity and saturation

For ultra-relativistic ions, the average ionization energy loss scales approximately as Z^2, motivating the study of the reconstructed LGAD response as a function of Z^2. Deviations from linearity are

2026 JINST 21 C04055

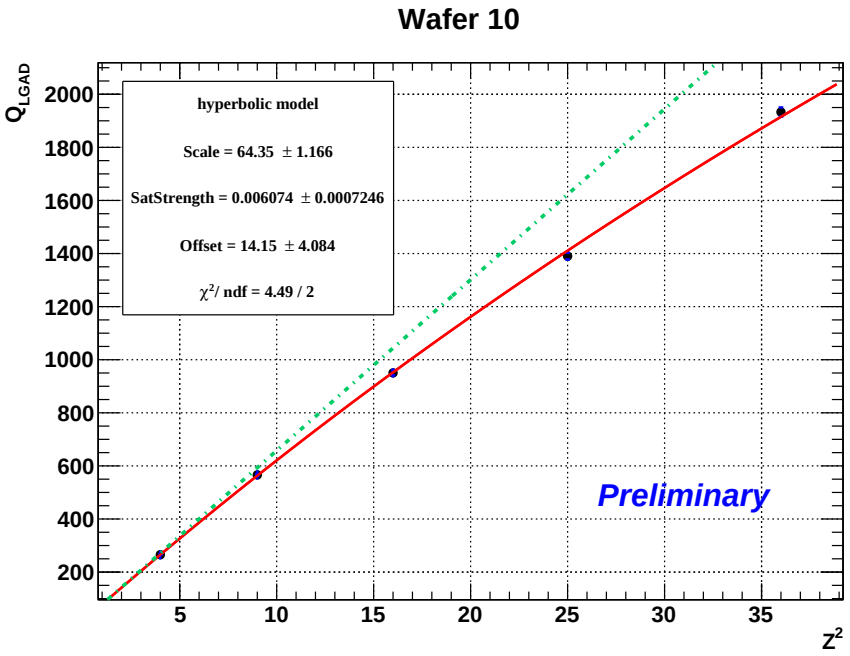

Figure 4. Reconstructed LGAD charge observable Q as a function of Z^2 for light ions (thick sensors). The red curve shows the best-fit empirical hyperbolic model of eq. (3.3), the dotted green curve is the linear part, illustrating the onset of saturation.

expected due to a combination of effects, including sensor gain saturation, charge-collection dynamics at high ionization density (quenching behavior).

We model the measured response with a simple empirical hyperbolic saturation curve:

$$Q(x) = Q_0 + \frac{A\,x}{1 + B\,x}, \qquad x \equiv Z^2, \tag{3.3}$$

where Q is the reconstructed LGAD charge observable, A sets the small-Z slope, B controls the saturation onset, and Q_0 represents the residual offset.

Figure 4 shows the thick-sensor trend for light nuclei and the best-fit model. Within the present statistical precision and Z coverage, the parameterization reproduces the departure from a purely linear Z^2 scaling while preserving good element separation. For the dataset shown, the fit yields (in the notation of eq. (3.3)) $A \simeq (64 \pm 1)$, $B \simeq (6.1 \pm 0.7) \times 10^{-3}$, and $Q_0 \simeq (14 \pm 4)$, with $\chi^2/\mathrm{ndf} \simeq 4.5/2$. In future campaigns and with further analysis refinements, the measurement will be extended to a broader Z range.

4 Timing performance

Timing measurements were performed using the dedicated BB boards instrumented for fast waveform acquisition. For each waveform, the baseline and leading-edge slope are extracted via linear fits, and the start time t_0 is defined as the intercept between baseline and slope, reducing time-walk effects by construction. The time difference between an upstream and a downstream pixel is computed event-by-event and fitted with a Gaussian; assuming comparable and uncorrelated contributions from the two channels, the single-pixel timing resolution is estimated as $\sigma_{\mathrm{res}} = \sigma_{\mathrm{fit}}/\sqrt{2}$.

2026 JINST 21 C04055

In the configuration discussed here (external trigger, $V_{\text{bias}} = 300$ V, thin sensors), the measured single-pixel timing resolution is at the level of $\sim$ 90–100 ps as reported in ref. [8], consistent with the project requirements for efficient rejection of late back-scattered signals.

A first timing evaluation of the ADA_5D v0 front-end chip was carried out using the discriminator output (COMP) with a BB board pixel as reference. After correcting time-walk via an amplitude-dependent calibration using the shaper output, the discriminator timing shows a resolution of order $\sim$ 220 ps in the studied configuration. While close to the design target, the result motivates further optimization of the next chip version, including a reduction of the shaper peaking time and improvement of the discriminator jitter. More details on the timing reconstruction and selections are reported in ref. [8].

5 Conclusions and outlook

The 2024 CERN SPS beam test successfully validated the ADA_5D concept, demonstrating that pixelated LGAD sensors can provide simultaneous position, charge, and timing measurements as required for high-energy direct cosmic ray measurements. For thick (275 µm) sensors, we achieved a single-layer charge resolution of $\sim$ 0.15 charge units for light nuclei and with a good separation power between adjacent elements, such as the 3.8 separation for He-Li.

On the timing side, BB board waveform acquisition achieved a single-pixel time resolution of 90–100 ps for thin sensors in the studied configuration. The ADA_5D front-end v0 prototype operated stably at the beam test; using the discriminator output with an amplitude-based time-walk correction, a resolution of order $\sim$ 220 ps was obtained, defining a clear optimization path for the next ASIC version.

The next steps are focused on extending the charge measurement to a broader Z interval, with bias- and rate-dependent scans to constrain saturation and disentangle sensor/electronics effects, in order to finalize the front-end design with reduced shaping time and improved discriminator jitter. Together, these activities will consolidate the scalability and low-power readiness of ADA_5D toward a large-area 5D detector for future space-borne cosmic-ray instruments.

Acknowledgments

We acknowledge the support of INFN and the ADA_5D collaboration, and thank CERN for the beam time allocation and support during operations.

References

[1] AMS collaboration, *Precision Measurement of the Helium Flux in Primary Cosmic Rays of Rigidities 1.9 GV to 3 TV with the Alpha Magnetic Spectrometer on the International Space Station*, *Phys. Rev. Lett.* **115** (2015) 211101.

[2] CALET collaboration, *Observation of Spectral Structures in the Flux of Cosmic-Ray Protons from 50 GeV to 60 TeV with the Calorimetric Electron Telescope on the International Space Station*, *Phys. Rev. Lett.* **129** (2022) 101102 [arXiv:2209.01302].

[3] CALET collaboration, *Direct Measurement of the Cosmic-Ray Helium Spectrum from 40 GeV to 250 TeV with the Calorimetric Electron Telescope on the International Space Station*, *Phys. Rev. Lett.* **130** (2023) 171002 [arXiv:2304.14699].

2026 JINST 21 C04055

[4] DAMPE collaboration, *Measurement of the cosmic-ray proton spectrum from 40 GeV to 100 TeV with the DAMPE satellite*, *Sci. Adv.* **5** (2019) eaax3793 [arXiv:1909.12860].

[5] P.S. Marrocchesi, *MOONRAY: A permanent high-energy cosmic-ray observatory on the surface of the Moon*, *Astropart. Phys.* **152** (2023) 102879.

[6] P.S. Marrocchesi, *A Cosmic Radiation Modular Telescope on the Moon: The MoonRay Concept*, *Particles* **8** (2025) 86.

[7] H.F.-W. Sadrozinski et al., *Ultra-fast silicon detectors (UFSD)*, *Nucl. Instrum. Meth. A* **831** (2016) 18.

[8] P. Brogi et al., *Beam test preliminary results of the ADA_5D LGADs Detectors and Front-End electronics*, 2025 *JINST* **20** C08032.

[9] M.G. Bagliesi et al., *A custom front-end ASIC for the readout and timing of 64 SiPM photosensors*, *Nucl. Phys. B Proc. Suppl.* **215** (2011) 344.

[10] S. Giroletti et al., *Analog Front-End for the Readout of LGAD-Based Particle Detectors*, *Nucl. Instrum. Meth. A* **1067** (2024) 169724.

[11] S. Giroletti, L. Ratti and C. Vacchi, *Pseudo-Differential Time-to-Amplitude Converter for LGAD Based Particle Detectors*, in the proceedings of the *2024 IEEE International Symposium on Circuits and Systems (ISCAS)*, Singapore, 19–22 May 2024, p. 1–5 [DOI:10.1109/iscas58744.2024.10558573].

2026 JINST 21 C04055